PREPRINTS

OF THE

STEWARD OBSERVATORY

THE UNIVERSITY OF ARIZONA

TUCSON, ARIZONA 85721, U.S.A.

Preprint No. 61

THE DEFINITION, VISIBILITY, AND SIGNIFICANCE OF REDSHIFT-MAGNITUDE BANDS

W. G. Tifft

Steward Observatory

University of Arizona

Tucson, Arizona 85721

Received 1973 June

ABSTRACT

Redshift-magnitude bands as they occur in the Coma cluster are formally defined and the original bands as observed in 1972 are shown to have a likelihood of random occurance of only 0.005 independent of their direction. The properties of the Coma bands are transformed to m_p magnitudes and used to show that an independent sample of outlying Coma galaxies shows strong band related characteristics. The properties of the Coma bands are then used to predict band properties for the A2199 cluster. The resultant power spectrum test of a preliminary A2199 sample shows agreement which has a random likelihood of occurance of only 0.001. The A2199 cluster also shows a band related morphological separation as in Coma.

INTRODUCTION

In a series of papers (Tifft 1972c CI, 1973a CII, 1973b QI) a new concept for interpretation of the redshift as a partially or entirely intrinsic property of matter has been introduced. Not surprisingly, the concept has not met with wide acceptance. The primary objection, aside from the qualitative resistance to any suggestion that new fundamental physics might be required, revolves about the statistical validity of the unexpected correlations found among the basic quantities redshift, luminosity (apparent magnitude), and morphology of galaxies and QSS objects. The principal objective of this paper is to examine the primary redshift-magnitude correlation and discuss the major arguments relating to its reality.

THE DEFINITION OF A REDSHIFT-MAGNITUDE BAND

Figure 1 shows the nuclear magnitude-redshift diagram of the original 70-point homogeneous statistical sample of galaxies in the Coma cluster core taken from CI. The diagram is the one from which the banding phenomenon was originally "recognized". The author has not found any significant number of persons who, presented with the diagram, fail to identify the characteristic band structure which slopes toward fainter magnitudes with increasing redshift at a rate close to 0.6 magnitude per 1000 km sec^{-1} of redshift. Subjectively, the bands are therefore quite clear although this is, of course, only a crude estimate of their actual statistical significance and is no assurance of their reality as a physical phenomenon. For reference purposes we shall refer to these bands as T bands which we shall subsequently attempt to specifically define.

Figure 1 contains a vector defining a direction which is closely aligned with the bands but which is independently defined by morphological separation and will be discussed later. This direction (0.64 magnitude per 1000 km sec^{-1} of redshift) will be taken as the direction in which a projected distribution is derived for statistical analysis. The method chosen for analysis is power spectrum as used in CII and QI. The specific form applied has distinct advantages of specifying no bins or boundaries which might influence the result. Such an analysis is, of course, attuned to periodic phenomenon, but this appears to offer little problem since we are dealing with an apparently reasonably periodic effect and deviations can only reduce the calculated significance. A power spectrum may fail to detect a significant effect but it should rarely overestimate its significance. Figure 2 contains the power spectrum of the Coma(70) distribution projected onto the redshift coordinate. It contains a power peak of 11.7 which has a likelihood (Table 6 of CII) of about 0.0005 of appearing in an unbiased random distribution of data points. The wavelength of the periodicity on the redshift scale is 1080 km sec^{-1}.

The author has frequently been confronted by the comment, occasionally accompanied by a diagram, which indicates that "bands" of one type or another are a common occurance in nature and should not be taken seriously. Upon examination of various examples, it has become increasingly obvious that "bands" may be defined in a variety of subjective and objective ways. Some objective formal definition of what is meant by a "band" must clearly be derived before any realisitic approach to interpretation of statistical significance is possible. One formal attempt at band definition, accompanied by an example, has been brought to the attention of this author. Figure 3 is a diagram taken from Barnothy (1973 BB) which contains "bands" in the direction of the vector shown. The figure is described as "a random sample displaying four very prominent bands." Barnothy and Barnothy define bands as being, or being produced by, a set of narrow fairly parallel linear voids through the diagram. Such a set of narrow voids (about $\frac{1}{3}$ the width of the intervoid "band") is in fact present in the indicated direction.

FIGURE 1

Redshift-nuclear magnitude diagram for the original CI Coma cluster investigation of 70 galaxies. The vector gives the direction of maximum morphological separation in the diagram, which agrees within 2° of the band direction. The bands in this diagram consist of parallel voids and ridges, that is, both strong negative and positive density fluctuations with respect to the average level.

(back of page 2)

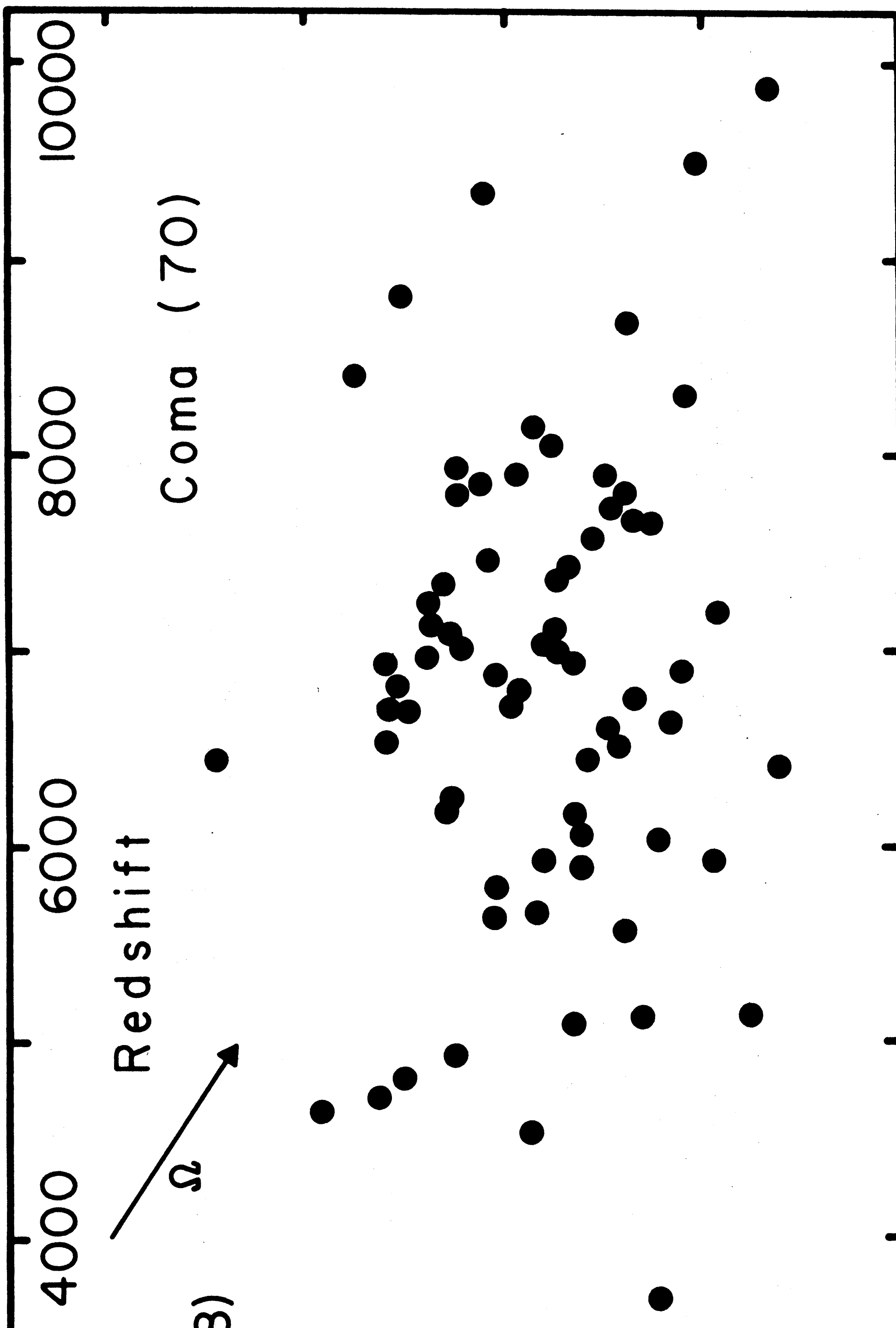

Coma (70)
Redshift
V(4.8)
Ω
4000
6000
8000
10000
14
15
16
17

FIGURE 2

The power spectrum of the Coma(70) distribution from Figure 1 projected in the direction of the morphological vector. The banding has a basic periodicity near 1080 km sec^{-1} and a likelihood of accidental occurance of 0.0005 to 0.005 depending upon whether the direction specification is included or excluded from consideration.

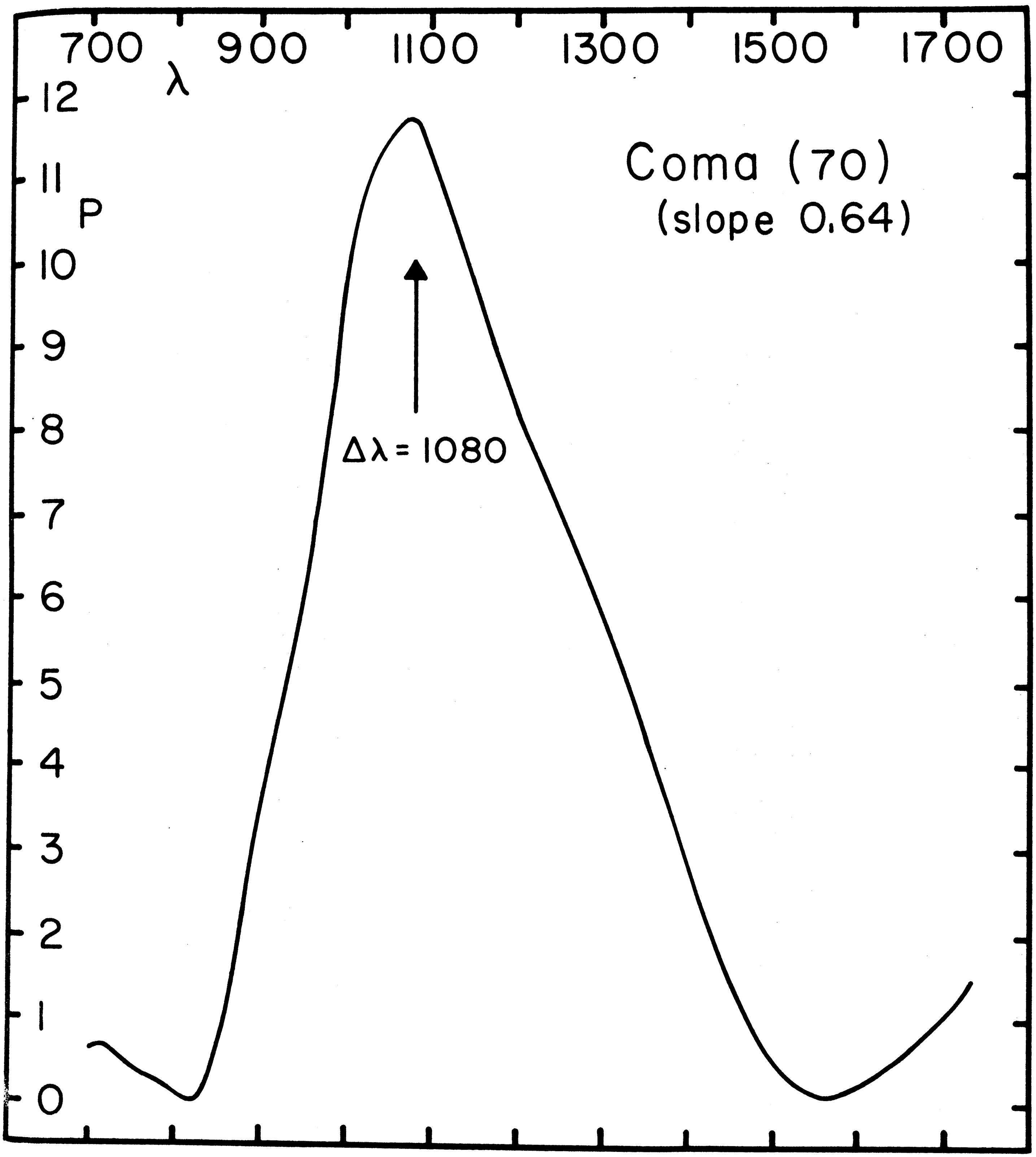
700
900
1100
1300
1500
1700
λ
12
11
10
9
8
7
6
5
4
3
2
1
0
P
Coma (70)
(slope 0.64)
Δλ = 1080

FIGURE 3

A randomized redshift-magnitude diagram taken from Barnothy and Barnothy (1973). This diagram contains a set of bands in the vectored direction. Unlike Figure 1, however, these bands are defined solely by narrow voids with a more or less uniform distribution of points between. Such bands are not statistically significant and are both subjectively and objectively quite different from the bands shown in Figure 1.

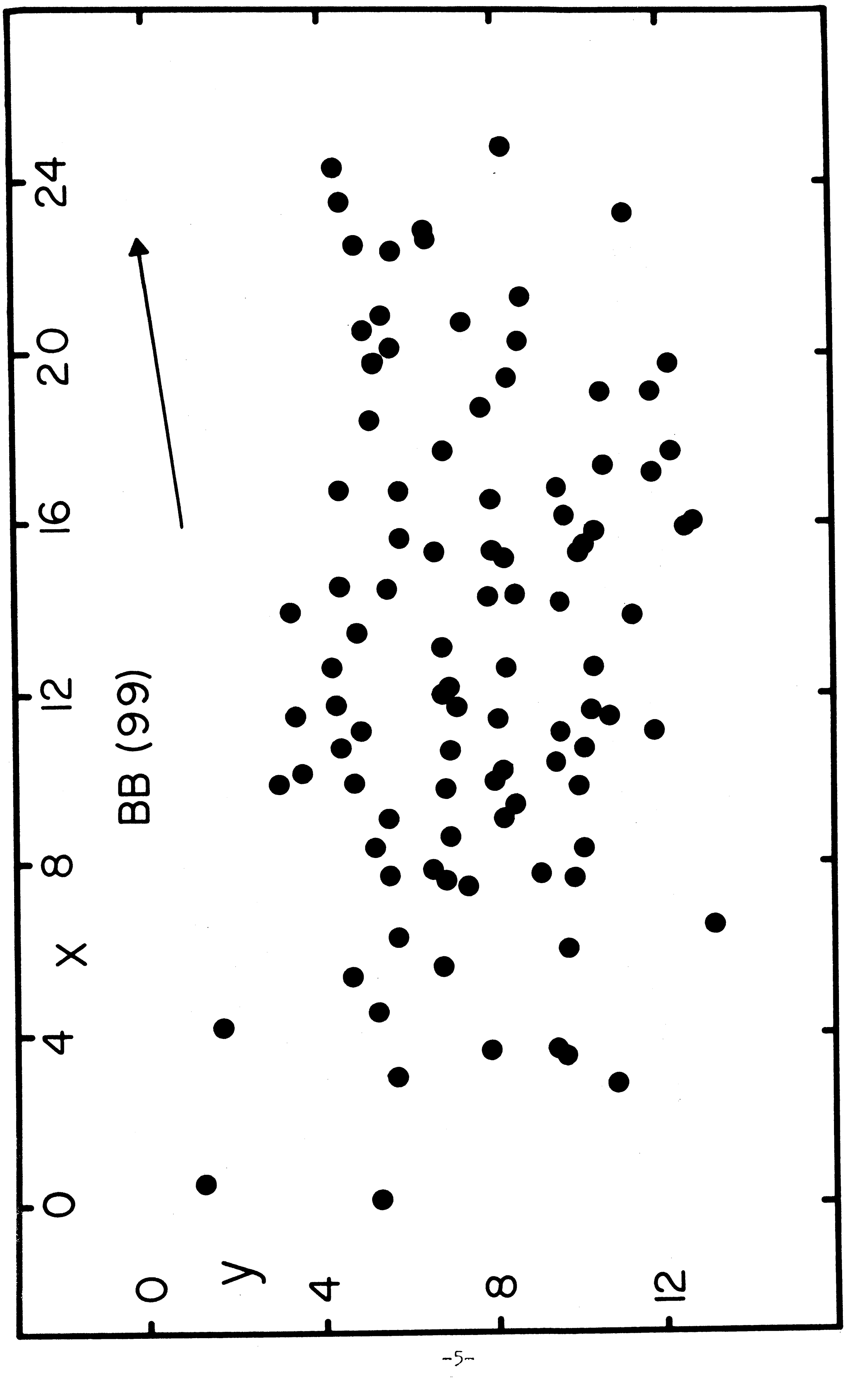
BB (99)
x
0
4
8
12
16
20
24
y
0
4
8
12

They calculate the probability of finding such bands in a 100-point sample as about 0.18 given no restrictions on orientation. Figure 4 is the power spectrum of the BB sample projected in the vectored direction. The power peak is about 5, which implies a probability of random occurance of about 0.4, in reasonable agreement with Barnothy and Barnothy.

As an interesting test in subjective band detection, Figure 3 was shown to the first ten faculty or graduate students encountered one morning at Steward Observatory. With the band direction vector masked off, no person saw the set of bands indicated, although there was a weak consensus for a marginal set of bands sloping downward toward the right. After the bands were demonstrated by card masking most persons still disclaimed to recognize them. Thus, it is obvious that both subjectively and objectively (power spectrum) the bands in Figure 3 are very different from Figure 1. For reference purposes we shall designate the bands defined by narrow parallel voids as B-B bands, which we shall subsequently formally define.

To resolve the great difference between the band visibility and significance in Figures 1 and 3 we must examine the point distribution between the B-B voids which both samples contain. Figure 5, therefore, presents the phase distribution of both patterns at their basic periods. Both sets of data contain roughly a 3σ deficiency of points in the B-B voids taken as phase 0.0. Between the voids, however, the BB(99) sample is essentially uniform, while the Coma(70) sample shows a narrow central 3σ ridge. The great subjective and objective difference between B-B bands and T bands is quite obviously due to this ridge which lies outside the definition of B-B bands, and is not accounted for in the BB probability calculation.

Unless the expected number of points in a narrow strip is very small, the likelihood of finding a set of voids (negative fluctuations) is not much different from the likelihood of ridges (positive fluctuations). We can, therefore, identify a class of bands which consist of narrow ridges on a more or less uniform background. We shall denote such bands as B+B bands and note that the probability of finding such a pattern must be reasonably similar to the probability of finding a B-B pattern. Barnothy and Barnothy (1973) give the probability of finding such a pattern in <u>any</u> orientation as 0.18 and since they con-

FIGURE 4

The power spectrum of the BB(99) distribution from Figure 3 projected in the direction of the vector shown. The periodicity produced by the narrow voids is significant only at the 0.3 level, hence this type of banding is very likely to be found in some direction in any two dimensional random distribution of points. This "banding" is quite different from that detected by the power spectrum analysis shown in Figure 2.

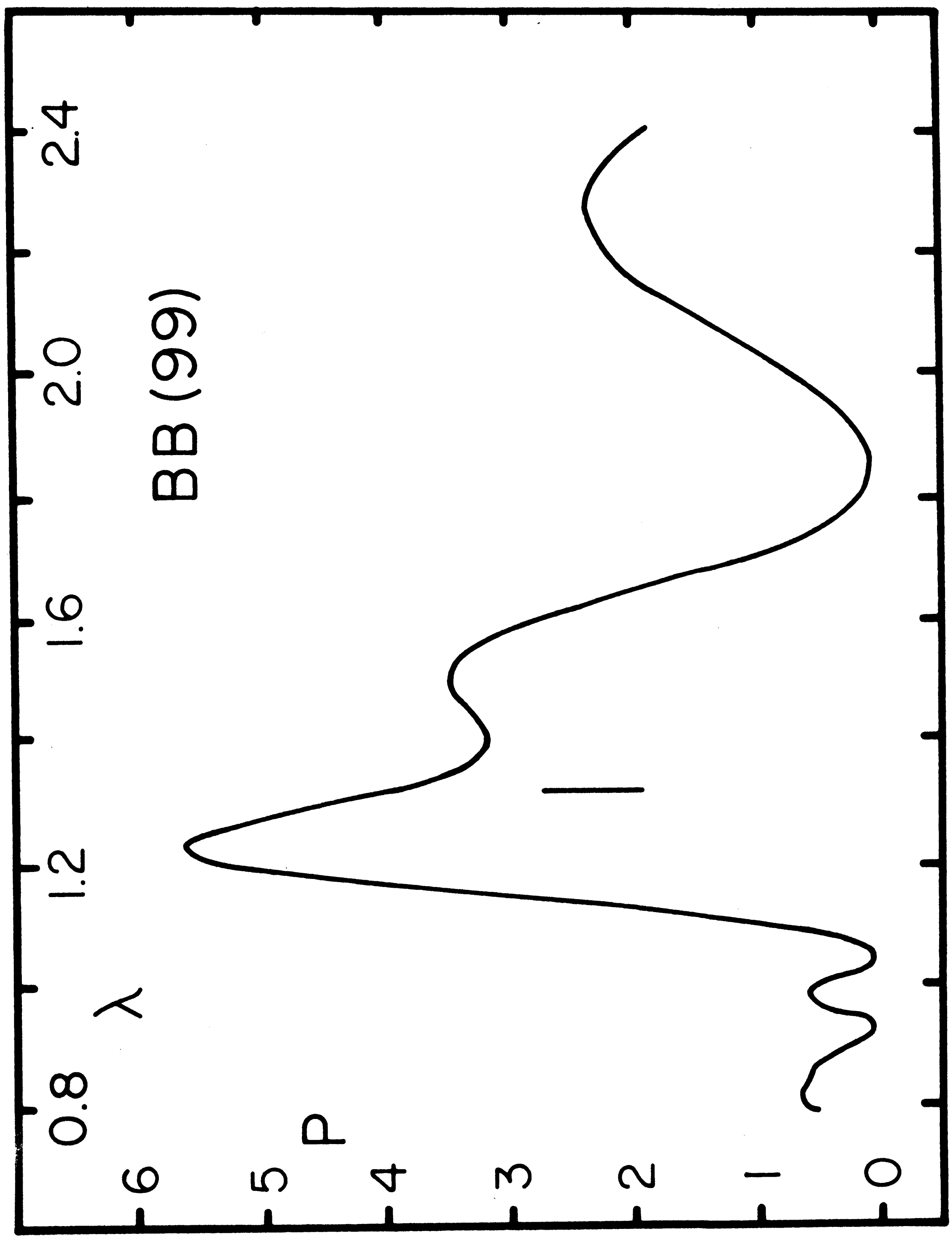
BB (99)
λ
0.8
1.2
1.6
2.0
2.4
P
0
1
2
3
4
5
6

FIGURE 5

The phase distribution of the points in the "bands" from Figure 1 (Coma) and Figure 3 (BB). A 1σ deviation is shown by the error bar. The Coma bands show strong positive as well as negative deviations from the average while the BB bands show only significant negative fluctuations. This difference explains the very different subjective and objective visibility and significance of the different types of bands.

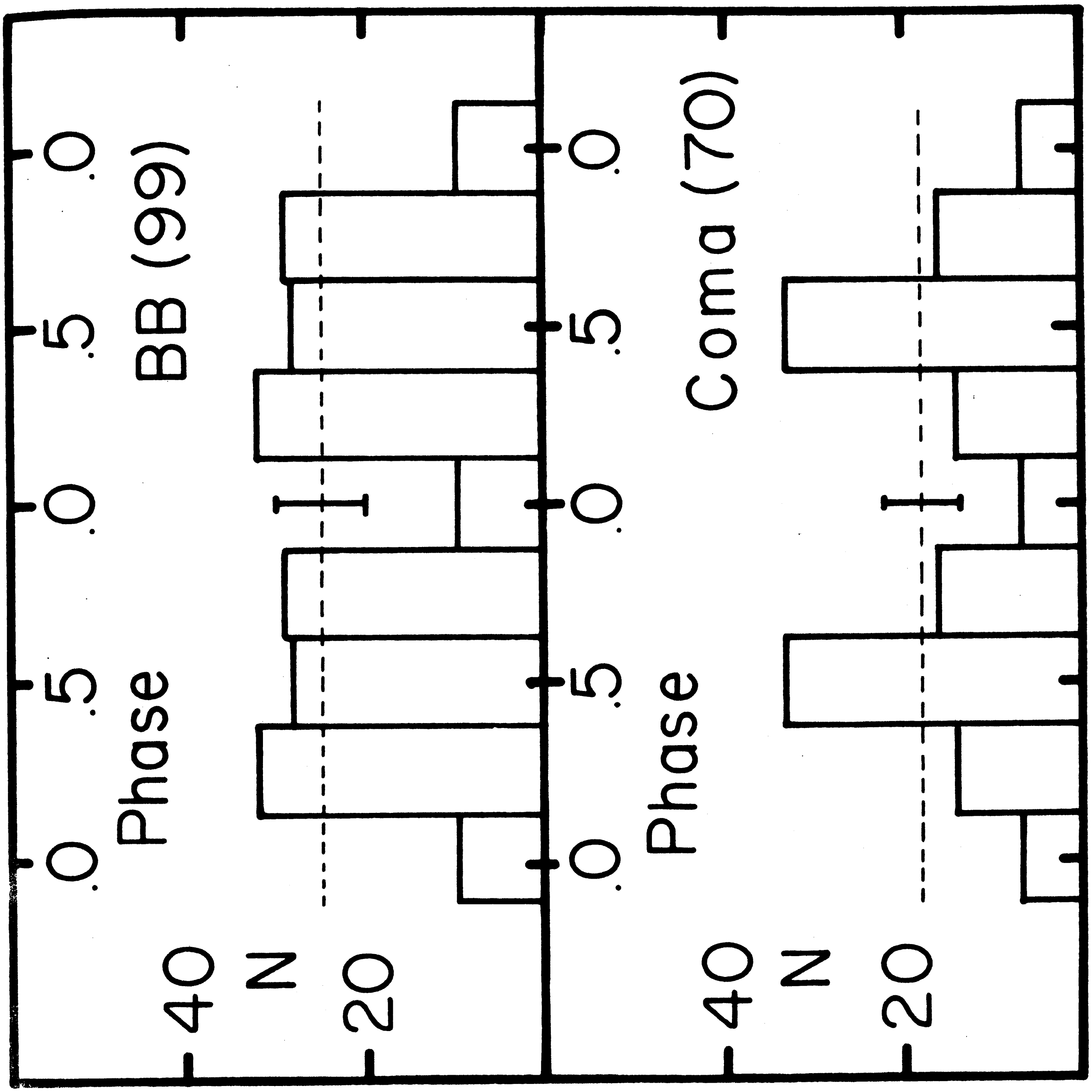
BB (99)
Coma (70)
Phase
Phase
N
N
40
20
40
20
0.0
.5
0.0
.5
0.0
0.0
.5
0.0
.5
0.0

sider that there are about 9 independent orientations of a pattern the probability of finding such a pattern in a specific orientation is about 0.02. We are now in a position to formally define bands and estimate their likelihoods of occurance.

> A B-B (B+B) band system consists of a set of narrow, semi-parallel approximately 3σ voids (ridges) through a two dimensional system of points and shows an essentially uniform point distribution between the voids (ridges).
>
> A T band system consists of a combination of a B-B band system aligned with a B+B band system.

The probability of occurance of a T band system in any direction in a two dimensional pattern is the product of the B-B system probability in any direction (0.18) and the B+B system probability in the direction defined by the B-B system (0.02) or 0.004.

The T band pattern in Figure 1 was shown to have the probability of random occurance of 0.0005 in the specific direction given by the morphological vector. According to Barnothy and Barnothy as noted earlier, such a diagram has about 9 independent orientations. The discussion in CI further confirms this figure, since strong banding appeared over a $\pm 7°$ orientation range which corresponds to 180/14=13 independent orientations. The T band pattern in Figure 1, therefore, has a probability of about 0.005 of being seen in any direction. The two estimates of the T band probability are essentially identical. Thus, there is no conflict between the likelihood of finding rather common B-B or B+B bands and the very unlikely and subjectively striking T bands.

THE BAND DIRECTION

One of the points most frequently raised in objecting to the band concept is that the high probability of non-randomness is contingent upon having a preferred direction specified. That is, the freedom to choose band direction degrades ones ability to calculate a meaningful probability. We have, however, seen in the previous section that such freedom can be allowed for, and in fact is not sufficient to destroy the significance of the result. The probability of finding the Coma(70) pattern is about 0.0005 if the direction specification is allowed and is still 0.005 if it is disallowed. If the agreement of the band and morphological directions is only by chance it has a probability of x/90 where x is the directional difference, in degrees, of the two correlations. From CI the band pattern and the morphological vector differ in direction by only 2° which, therefore, has a chance likelihood of occurance of only 0.02.

The author has heard on several occasions the statement that there are many correlations possible among the observable quantities and by searching among them one can easily choose one which will match the band direction purely by accident. In fact, there are only about three other parameters which could be substituted for morphology to define a direction. These are diameter, distance from cluster center, and major axis orientation. Other properties which might be used are simply not available; for example color or internal velocity dispersion, or are available for very few objects; for example radio source information. Some parameters are too coarse to use; for example spectral type, or are not independent; for example ellipticity and morphology.

Among the possible parameters mentioned for redshift correlation, only magnitude, morphology and diameter are intrinsic variables. Diameter is far less independent of magnitude than is morphology, thus one might replace magnitude with diameter but not logically replace morphology. Correlations with extrinsic variables of position or orientation are secondary effects which have less bearing on the main thesis which is the possible interpretation of redshift as an intrinsic variable. Thus, in fact, the only correlations which give clearly independent results among the available intrinsic variables are the ones used, m-Vo, m-morphology, and Vo-morphology.

Finally, a certain amount of physical logic applies to the choice of variables. Having a suggestion from the m-Vo diagram that a discrete or "quantized" effect is present one could scarcely choose a more likely variable than angular momentum (morphology or ellipticity) to examine separately with respect to m and Vo. The Vo-morphology separation alone is significant at the 0.01 level by Students' t testing discussed in CI.

SAMPLE EQUIVALENCE

Despite the presence of the three unexpected significant correlations in the Coma cluster, the best test comes from verification by observation of an independent sample of galaxies. One version of such a test is provided in the final section of this paper. Another version has been proposed by Barnothy and Barnothy (1973). In order for such tests to be valid they must be applied to a data sample as equivalent as possible to the original Coma sample. The same type of magnitude should be employed, the same portion of the luminosity function must be used, and similar spatial regions of a cluster should be considered. The average redshift of the sample should be as close as possible to the Coma redshift, and, if possible, sample completeness or selection effects should be similar.

The band phenomenon is a property of nuclear magnitudes and while it can be seen to some degree in total magnitudes as shown in CII it is unlikely that it would be initially recognized with such magnitudes. A combination of secondary effects, such as dust effects and star formation, in the outer portions of galaxies, coupled with lower photometric accuracy and unknown effects simply superimposes too much scatter on the pattern to make it readily visible. Whatever the underlying fundamental variable may be, which is being "represented" by nuclear magnitude, it apparently is a property of galaxy nuclei. Magnitude is only an estimator of a more fundamental property such as nuclear mass or energy which very likely plays a central role in galaxy origin and evolution. Just as in the physics laboratory, conditions must be controlled or restricted to emphasize the visibility of a particular effect, so with redshift-magnitude banding in galaxies the presently available best estimator is nuclear magnitude. Insistance that the effect, to be real, must be readily seen in total magnitudes will not make the nuclear magnitude correlation disappear! In the recent paper by Barnothy and Barnothy (1973) a sample of galaxies in the Coma region which has been studied by Rood, Page, Kintner, and King (RPKK, 1972) was considered. The only magnitudes available for these galaxies are m_p values which are considerably less accurate than the V_{26} isophotal magnitude in the inner region given by Rood (1969). The V_{26} isophotal magnitudes already degrade band detection so that the power spectrum analysis detects the bands at a power level of only 7. If the bands were not known to be there, a power level at 7 would imply only an 0.1 likelihood that the distribution is non-random. To degrade magnitudes still further will render bands with the Coma spacings quite clearly indetectable. Thus, if the RPKK sample contains band information, it would not be expected to be detectable as visible bands and cannot constitute a test for the effect. The weak "bands" which Barnothy and Barnothy (1973) suggest to be present in the RPKK sample and which run perpendicular to the bands defined in CI and CII are presented without statistical support. They are of the general B-B band type and appear to have no significance.

There is nothing in the band phenomenon which requires that it extend uniformly or in the same form throughout the entire luminosity function of a cluster. The basic band system could, for example, play a role analogous to the stellar main sequence from which giant or supergiant and other special classes of stars evolve to populate different portions of the luminosity function. The RPKK sample investigated by Barnothy and Barnothy only slightly overlaps the CI and CII samples in luminosity. Even if the magnitudes were sufficient to detect a band system or if the different band system suggested in BB were real, the RPKK sample contains little information equivalent to the CI and CII samples, and can, therefore, at most extend, not contradict, CI and CII.

In addition to representing a different portion of the luminosity function, the RPKK data is derived from a different portion of the Coma cluster spatially. The CI and CII galaxies lie within $0.^\circ4$ of the cluster center, while the RPKK sample extends outward to 4°. It is known that there are changes in the luminosity function with radius (Rood, 1969) and changes in the incidence of emission lines with radius (Chincarini and Rood, 1972c, Tifft and Gregory, 1973). Spiral galaxies increase in frequency with radius and there are variations in the redshift distribution with radius according to RPKK. Thus there is no reason to expect an identical redshift-magnitude diagram with radius; and in fact, some changes must occur. Much more data must be obtained on galaxies as a function of radius to understand what effects may be present. A program to extend the faint Coma sample by a slight increase in radius from $0.^\circ4$ to $0.^\circ5$ is in progress; however, at present it is not established that even such small radial extensions produce equivalent samples.

Finally, in addition to magnitude, luminosity function, and spatial differences, the RPKK sample is incomplete and inhomogeneous with respect to limiting magnitude, spatial sampling, and morphological content. It is difficult to precisely assess factors of incompleteness and corrections for field contamination. It is, therefore, difficult to predict what patterns might be found within the sample itself if the factors were changed, and certainly difficult to apply any results to the faint core region of the cluster. In conclusion, the RPKK sample is non-equivalent to the Coma core sample in so many respects as to permit few useful tests for the direct visibility of the band phenomenon as defined in CI and CII.

BAND RELATED MORPHOLOGY

Although the RPKK sample of galaxies provides little if any useful direct visible information on redshift-magnitude bands it does contain important information on the relationship of galaxy morphology to the bands. In CI and CII it was shown that morphology varies systematically along each band. The RPKK sample contains an appreciable number of galaxies which must lie near the upper end of the three prominent bands, hence any morphological properties of the "ends" of the bands might be expected to be visible. Subdivision of the sample into morphological subgroups was therefore tried as a possible means of making the bands "visible" and was originally reported at the Seattle AAS meeting (Tifft, 1972a).

As a first step, the general location of the bands in a m_p-Vo diagram must be determined, even though they are not directly visible. This has been done by plotting the general m_p-Vo diagram for the RPKK sample (omitting double galaxies, galaxies with Vo<3500 or Vo>10000, and galaxies with m_p>15.7). This list was supplemented by other galaxies in CI and CII which have m_p values given by Zwicky and Herzog (1963), the list of galaxies in the Coma region given by Tifft and Gregory (1973), and galaxies in the Chincarini and Rood (1972a, 1972b) lists within 6° of the Coma cluster. Table 1 gives a summary of the sources and morphological properties of the sample which includes 143 galaxies. By means of the objects in common between the m_p list and CI or CII the general location of the three principal bands can be inferred and is shown in Figure 6. Galaxies of types E, SO, and SBO have been used. Each galaxy is plotted as a numerical symbol corresponding to the band membership assigned in CI and CII and a set of band location lines has been drawn to represent the points and to gener-

FIGURE 6

The m_p-redshift diagram of E, SO, and SBO galaxies in the central region of the Coma cluster which are in common between CI and CII and this investigation. The symbols indicate band identity from CI or CII. The lines represent the mean location of the Coma bands in the m_p-Vo diagram drawn to represent the points and satisfy other general spacing and convergence properties. The two central Coma cluster supergiant galaxies are shown with crosses.

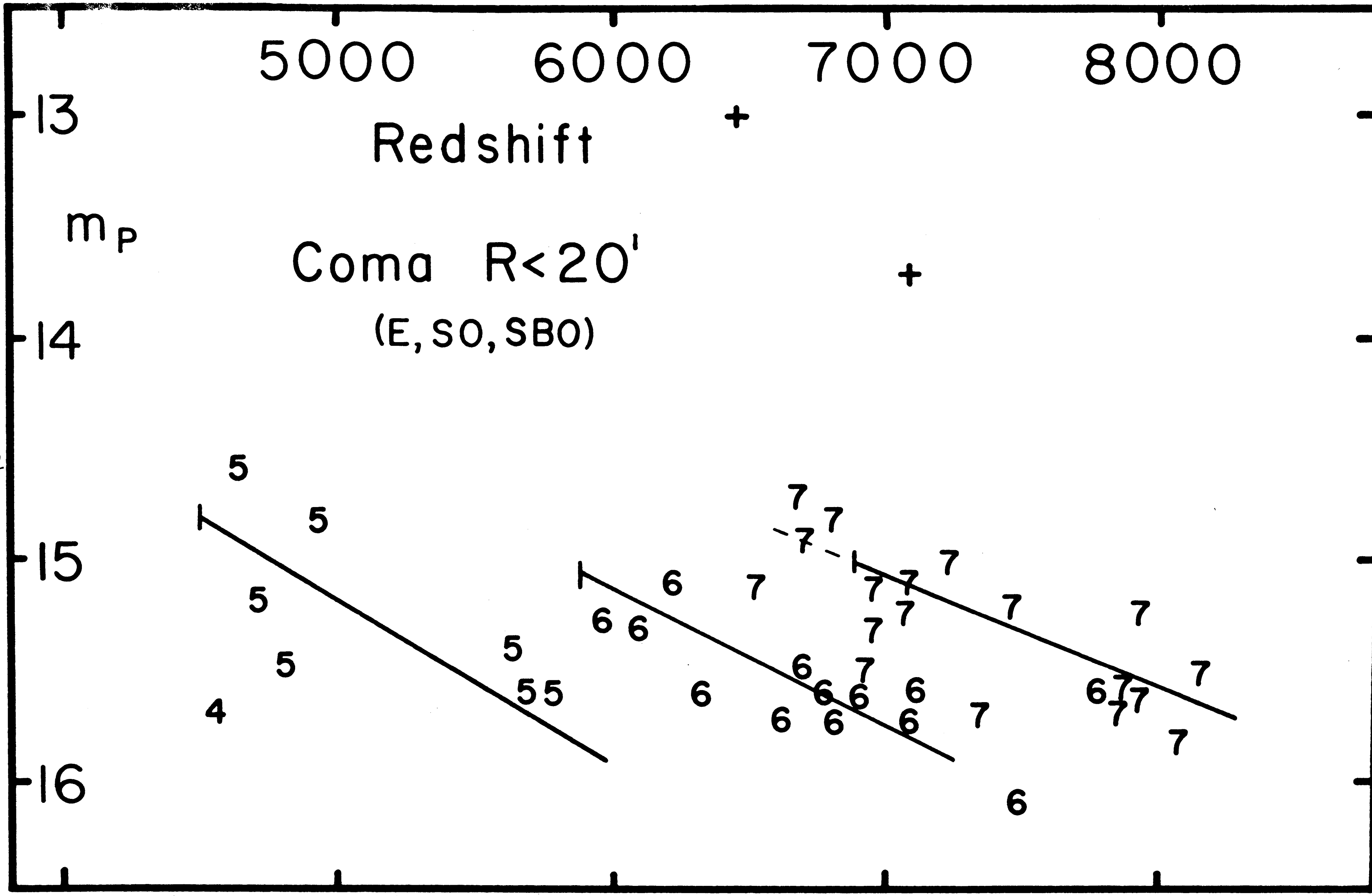

5000
6000
7000
8000
13
14
15
16
m_P
Redshift
Coma R<20'
(E, SO, SBO)

ally satisfy the known band spacings and the convergance to zero redshift. A new band numbering notation equal to nine minus the old notation is used. The newer notation will be defined in detail and used in subsequent papers.

TABLE 1

Properties of the Extended Coma Sample, R<6°

Data Sources

References	Galaxies Accepted	Galaxies Rejected: Doubles	Vo<3500	Vo>10000	m_p>15.7	Duplicates
RPKK	93	7(1)	11	1	5	
CI, CII	17	1*			51	38
Tifft and Gregory (1973)	21	1	1	2		2
Chincarini and Rood (1972a, b)	12	1*				19

Morphology and Radial Distribution

Type	R<20'	R>20'
Non-emission line E	23(1)	28(2)
Non-emission line SO	13(1)	21(2)
Non-emission line "others"	12(1)	12
Emission line objects	1(1)	25(1)
Unclassified		8

* redshifts given for both components, magnitude for pair
( ) gives number of 5C radio sources in each category (Willson, 1972)

The redshift distribution of the total m_p(143) data sample is relatively smooth; it shows no obvious effects of the band pattern which is as expected since the bands slope across the redshift coordinate. Figure 7 is the general m_p(143) redshift-magnitude diagram shown with no markings. The figure shows no obvious "bands", which is also expected as noted previously. For the purpose of analysis we shall consider the m_p(143) sample in two radial zones, R<20' and R>20' and in several morphological subgroups as summarized in Table 1. The R<20'

FIGURE 7

The m_p-redshift diagram for 143 galaxies within 6° of the Coma cluster center. As discussed in the text, when viewed in this form no unusual properties are visible.

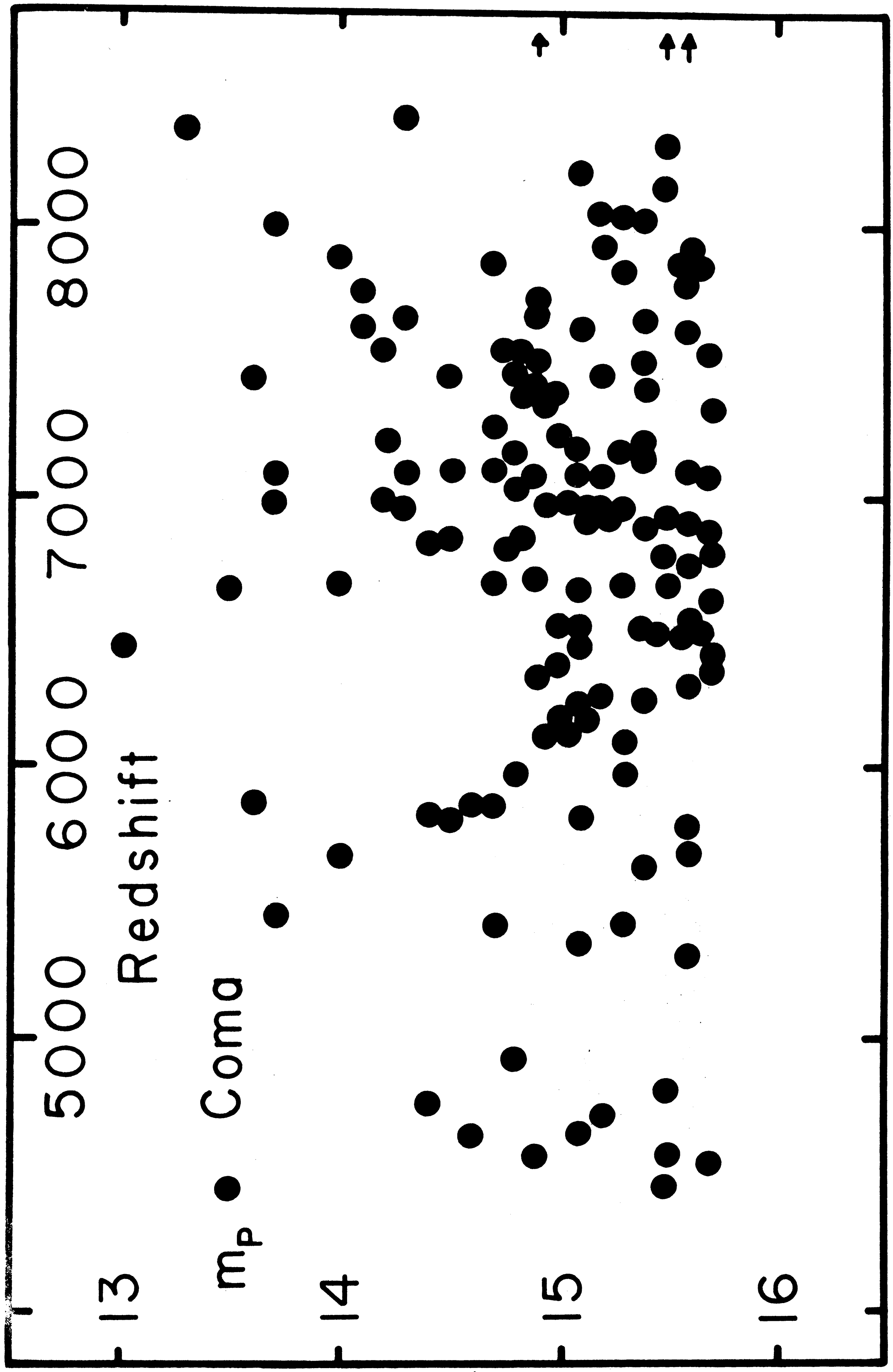

Redshift
Coma
m_P
5000
6000
7000
8000
13
14
15
16

sample of 49 galaxies contains only four galaxies which were not in the CI or CII analysis (they fall in the few gaps present in the Rood and Baum, 1967, survey), hence its properties are "known". The R>20' sample of 94 galaxies contains only three galaxies which were in the CI or CII study, hence its properties are "unknown" and it will provide a test sample.

The average band spacing in the redshift coordinate of the Coma cluster is near 1080 km sec^{-1} as was seen in the power spectrum analysis in Figure 2 or can be calculated from Table 2 of CI. We shall ignore here any effects of variation in band spacing or convergance effects as second order and ask only if we can detect the basic 1080 km sec^{-1} redshift periodicity in the m_p(143) sample or its various radial and morphological subsets. We note that in a power spectrum analysis at a single frequency the probability of finding a given power level P for a random assembly of points is e^{-P} (Lake and Roeder, 1972 Burbidge and Odell, 1972). Thus, when the properties of a sample are fully predicted, a large power peak is not required for significance. When searching over a wide frequency interval, a peak must be high to be significant (Table 6 of CII) since we have introduced many degrees of freedom (i.e. the number of frequencies studied, which we have generally taken to be approximately equivalent to the number of data points in the sample since the probability varies only slowly once the number of points is large).

If we consider a restricted magnitude interval in a banded redshift-magnitude diagram, the redshift values in that interval should show the characteristic redshift periodicity of the banding since we have minimized the blurring produced by the sloping and overlapping of the bands. Likewise, if morphology varies systematically along the bands, by choosing specific morphological classes we might expect to isolate specific "sections" of bands. By restricting both magnitude and morpholgy we might expect to "see" the bands even though the complete pattern has inherently quite a high scatter. We will illustrate this first with the "known" m_p(R<20') sample of data. From the CI and CII studies the morphology is known to vary along the bands. Following CI we therefore isolate two morphological classes, E and non-E galaxies, and limit the magnitude interval to $14.5 \le m_p \le 15.7$. We <u>predict</u> that a power spectrum analysis of these subsets of data will show a periodicity of 1080 km sec^{-1}. The two power spectra are illustrated in Figure 8 and the results summarized in Table 2 in the form of power and probability at the predicted wavelength. It is apparent that in the non-E sample a significant power is present at the predicted wavelength, and an actual power peak is present within ten percent of the predicted wavelength. Since only a few cycles defined by noisey data are present it is not surprising to find some shift in the peak wavelength. The banding predicted periodicity is, however, "visible". The E galaxies show a small peak at the predicted wavelength and a powerful peak close to twice the wavelength. Inspection of the data sample shows that nearly all the points lie on one band with very few on the middle band. The strongest periodicity is therefore set by the two widest spaced bands. Since the periodicities found were "known" to be present, the probabilities in Table 2 have little meaning. We are now in a position, however, to examine the "unknown" independent outer sample where the prediction has full significance.

TABLE 2

Inner Coma Sample Analysis

Subsample	Wavelength	P	e^{-P}
non-E(23)	1080	3.2	0.04
	1150 (peak)	4.2	0.015
E(22)	1080	1.8	0.17
	1040 (peak)	2.0	0.14
	2160	5.9	0.003

In the magnitude interval 14.5-15.7 the outer Coma sample contains enough galaxies to define two morphological subgroups of population 20 or greater which cover a wide redshift interval. The first calss contains 20 ordinary non-emission SO galaxies. Among the remaining galaxies a strikingly high frequency of emission line objects are present and a class of galaxies defined purely by the presence of emission lines was made containing 22 galaxies. Fifteen E galaxies, eight non-emission spiral types and six unclassified absorption line galaxies complete the list. The last two form too small or inhomogeneous groups for testing.

FIGURE 8

Power spectra of the redshift distribution of inner Coma E and non-E galaxies in the $14.5<m_p<15.7$ range. The basic band periodicity near 1080 km sec^{-1} is readily seen. In the case of the E galaxies which clump strongly to one band, most of the power is concentrated in the 2λ peak.

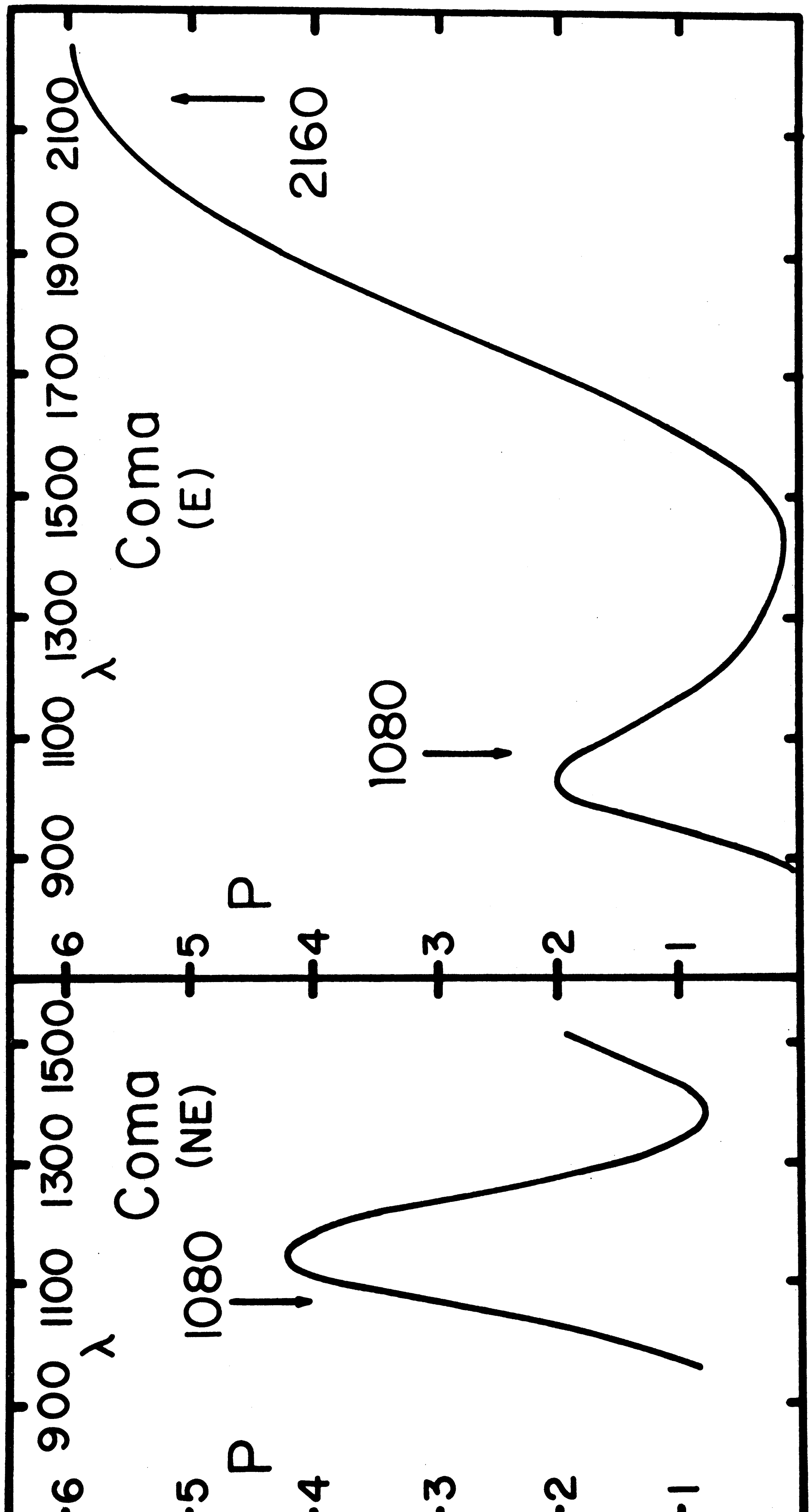
Coma
(E)
Coma
(NE)
1080
1080
2160
P
P
λ
λ
900
1100
1300
1500
1700
1900
2100
1
2
3
4
5
6

As with the inner E types, the E galaxies concentrate in a narrow redshift range (barely 1700 km sec^{-1}) which is not adequate to define a distinct period. The meaning of a power spectrum analysis breaks down as the wavelength approaches the total sample interval. Table 3 contains the power spectrum analysis of the two well defined outer Coma subsets in the same format as Table 2. Both samples show a well defined periodicity at the predicted wavelength, more striking than the "known" inner Coma effect. Either one alone has a likelihood of accidental occurance of only a few percent. The likelihood of two such occurances is small indeed.

TABLE 3

Outer Coma Sample Analysis

Subsample	Wavelength	P	e^{-P}
SO(20)	1080	3.6	.03
	1200 (peak)	4.2	.015
Emm(22)	1080	3.9	.02
	1000 (peak)	4.5	.01

The band associated morphological periodicity in the outer Coma data is so striking that it is quite easily visible in a normal redshift-magnitude diagram. Figure 9 is the redshift-magnitude diagram of the complete outer SO sample. The band locations as defined previously are shown. A small circular region has been drawn near the upper end of each band. These three small zones contain all but four of the SO galaxies. One region is apparently associated with each band. In Figure 10 the emission line galaxies are shown. The band locations and SO reference circles are repeated from Figure 9. The band association of the galaxies is quite clear with systematic displacement down along each band from the SO populated regions. Note that if the SO and emission line galaxies were not separated morphologically they would essentially completely mask the bands since their periodicity is shifted in phase close to one half period. This outer sample analysis would seem to show that not only are the bands fairly certainly present, but they show the same type of morphological gradation along them as do the

FIGURE 9

The m_p-redshift diagram for SO galaxies outside the core region of the Coma cluster. The galaxies concentrate in three band-associated regions which become visible when morphological types are isolated. The band lines are shown as defined in Figure 6.

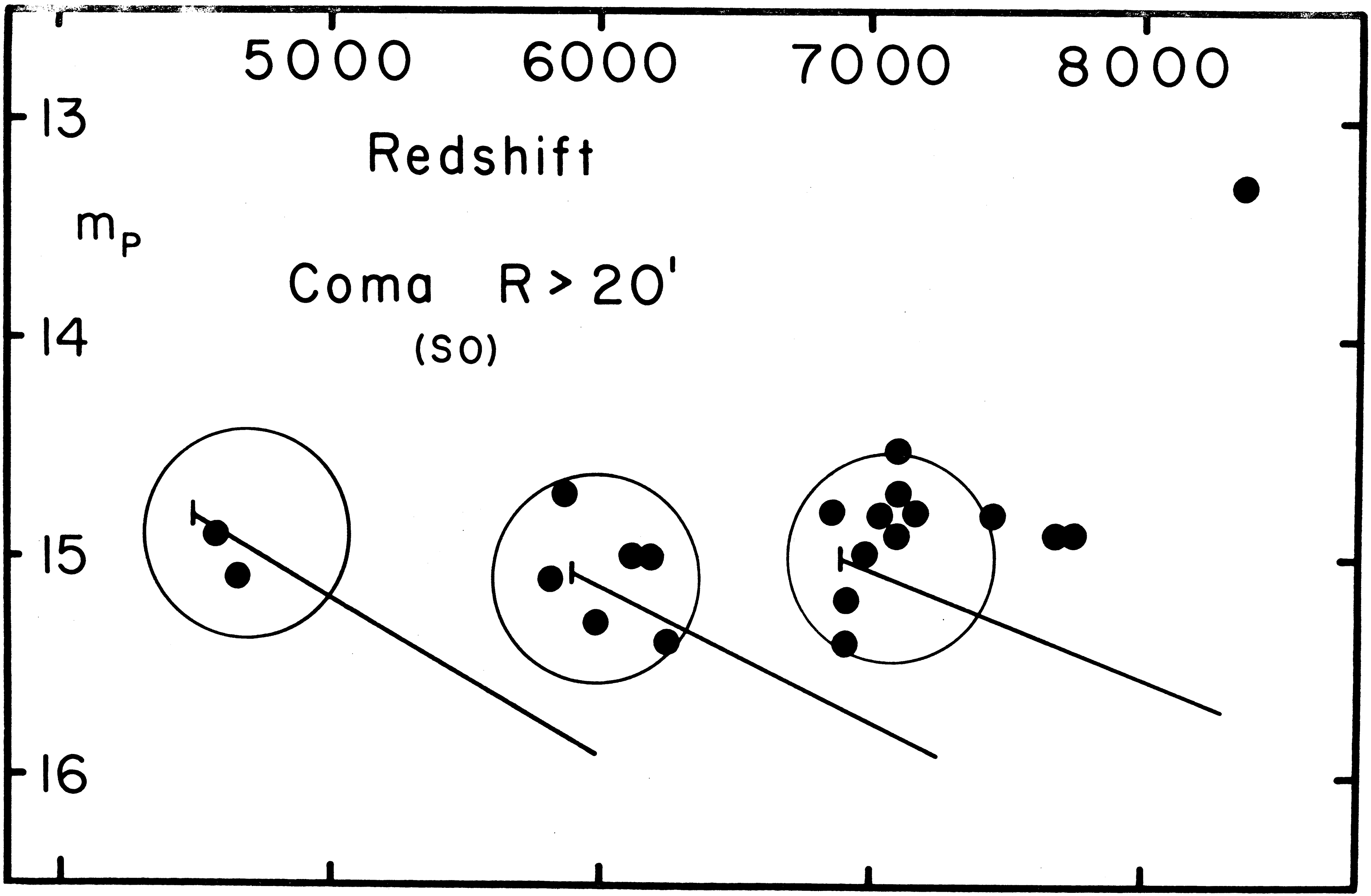
5000
6000
7000
8000
13
14
15
16
m_P
Redshift
Coma R > 20'
(SO)

FIGURE 10

The m_p-redshift diagram for Coma cluster galaxies showing emission lines. All galaxies lie outside the cluster core region except the one shown with an open circle. The band lines are shown as defined in Figure 6. The three circles within which SO galaxies concentrate are shown from Figure 8. The galaxies concentrate in band associated region systematically shifted from the SO regions. The dashed band extensions are shown to indicate a possible association of bright galaxies in the cluster with the ends of the bands.

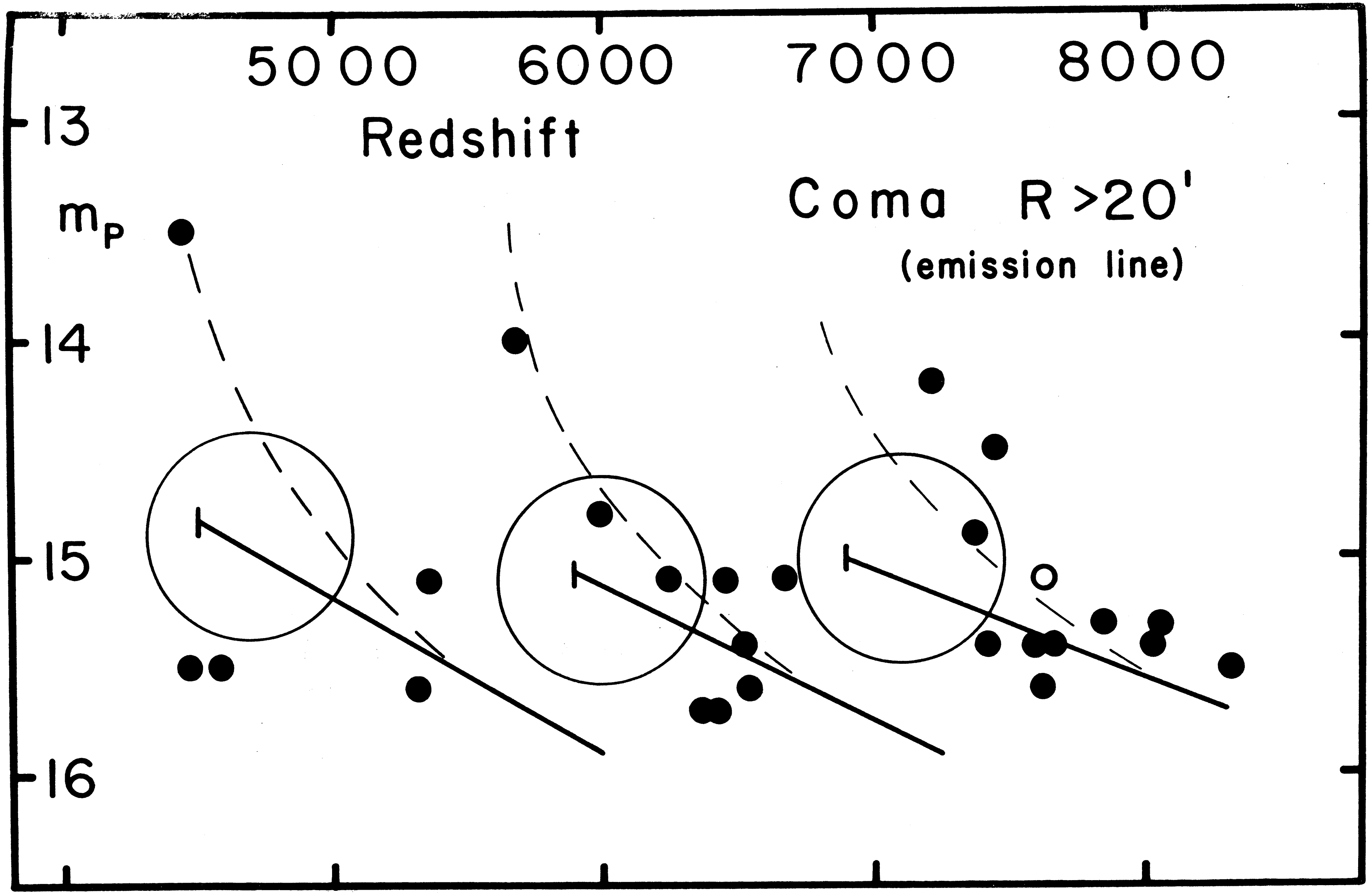
5000
6000
7000
8000
13
14
15
16
Redshift
m_P
Coma R >20'
(emission line)

bands in the inner sample. One new result would seem to be that in addition to trending toward later types along each band, there is a trend toward later types at any given point on a band as one goes outward in the cluster.

While a good case can be made for associating galaxies below about m_p=14.5 with the known bands, this does not explain the galaxies that lie above m_p=14.5. They might, of course, represent fragments of higher bands. Alternatively, Figure 10 contains three upward curving dashed lines connected to the known bands; it is suggested that most of the brighter galaxies associated with such band extensions, at least those with redshifts less than about 7200 km sec^{-1}. Figure 11 shows the outer E galaxy sample which indicates some support for such an upward extension of the bands as does the very limited spiral galaxy sample. Finally, Figure 12 is the entire m_p(143) diagram repeated from Figure 7 with the addition of the band location lines and the upward curving extensions. While it is premature to be certain of such an extension it is interesting that a power spectrum of the 29 points of m_p=14.5 or brighter shows a power peak, close to the 1080 wavelength, with a likelihood level of only 0.08 of randomness.

One remaining unusual morphological separation is present in the m_p(143) galaxies. Figure 13 illustrates the location of the 10 identified 5C radio sources (Willson 1970). One of these, shown as an open circle, is from the double galaxy reject list, hence its magnitude is uncertain; however, only the redshift will concern us here. Nine of the ten galaxies lie above the mean redshift of the cluster. The likelihood of this happening by accident can be evaluated by a two cell χ^2 test or simply as the equivalent of a run of heads or tails in coin tossing and is in the neighborhood of 0.01. A formal Students' t test gives t=2.2, p=0.01. The difference in the mean redshift of the entire sample (6820) and the 5C radio sources (7470) is 650 km sec^{-1}. While the relationship of this phenomenon to the bands is obscure, since they occupy the one region of the m-Vo diagram which is <u>not</u> obviously banded, they present another distinct case against the classical dynamical redshift interpretation. Note that the 5C sources are not at all similar in morphology. Since these galaxies are high redshift bright objects, the discordant redshift cannot be easily explained as an effect of background objects.

FIGURE 11

The m_p-redshift diagram for Coma cluster E galaxies outside the core region of the cluster. The two central supergiant galaxies are also indicated by crosses. Reference lines are as shown as in Figure 10 and previous figures. The E galaxies show some tendancy to populate the dashed band extension lines and tend to avoid low redshifts and populate the bright high redshift corner of the diagram.

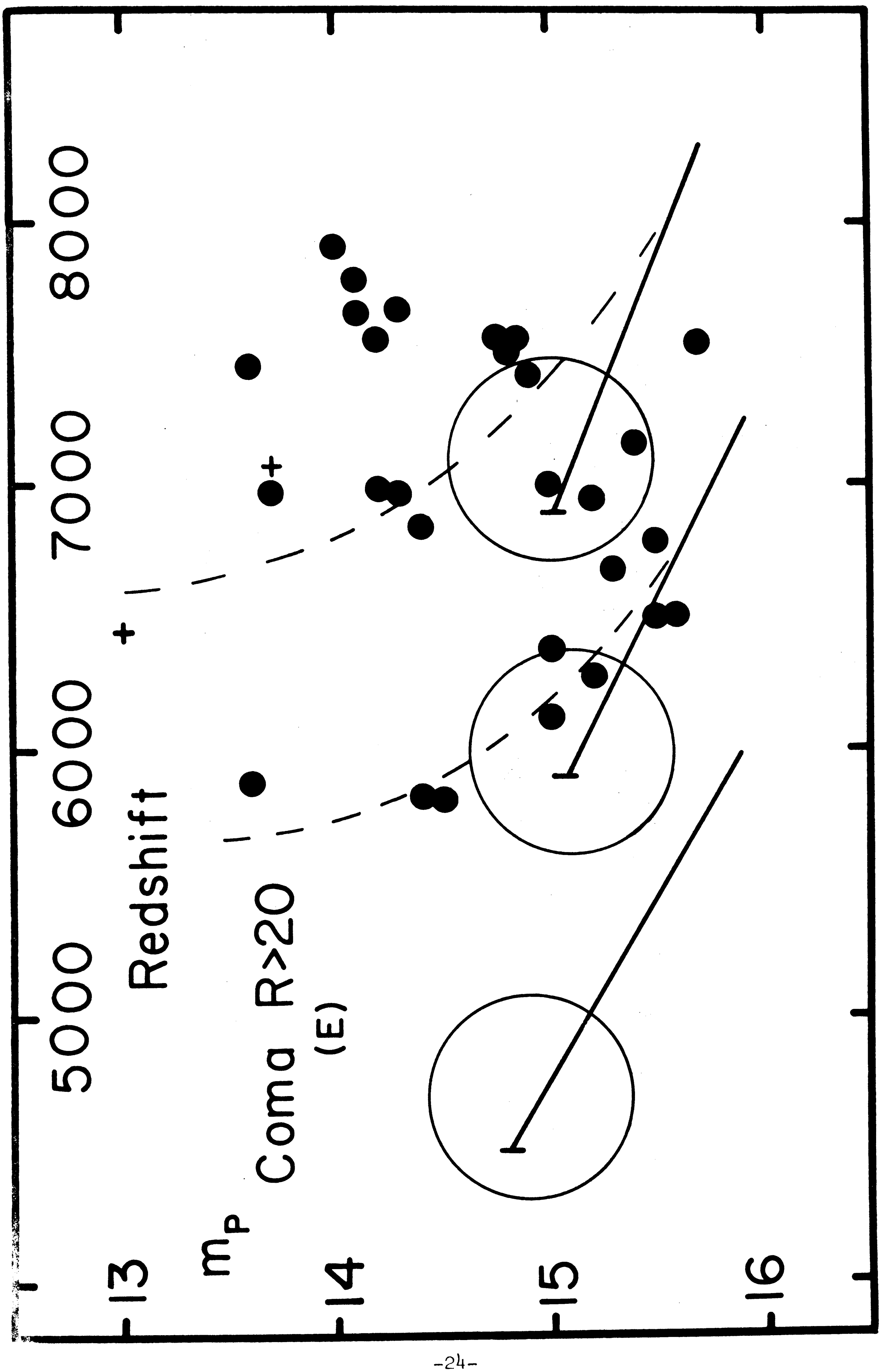

Redshift
50000
60000
70000
80000
m_P
13
14
15
16
Coma R>20
(E)

FIGURE 12

The m_p-redshift diagram for 143 galaxies within 6° of the Coma cluster center. This is a repeat of Figure 7 with band lines shown. The general tendancy for bright galaxies to populate the band extensions can be seen.

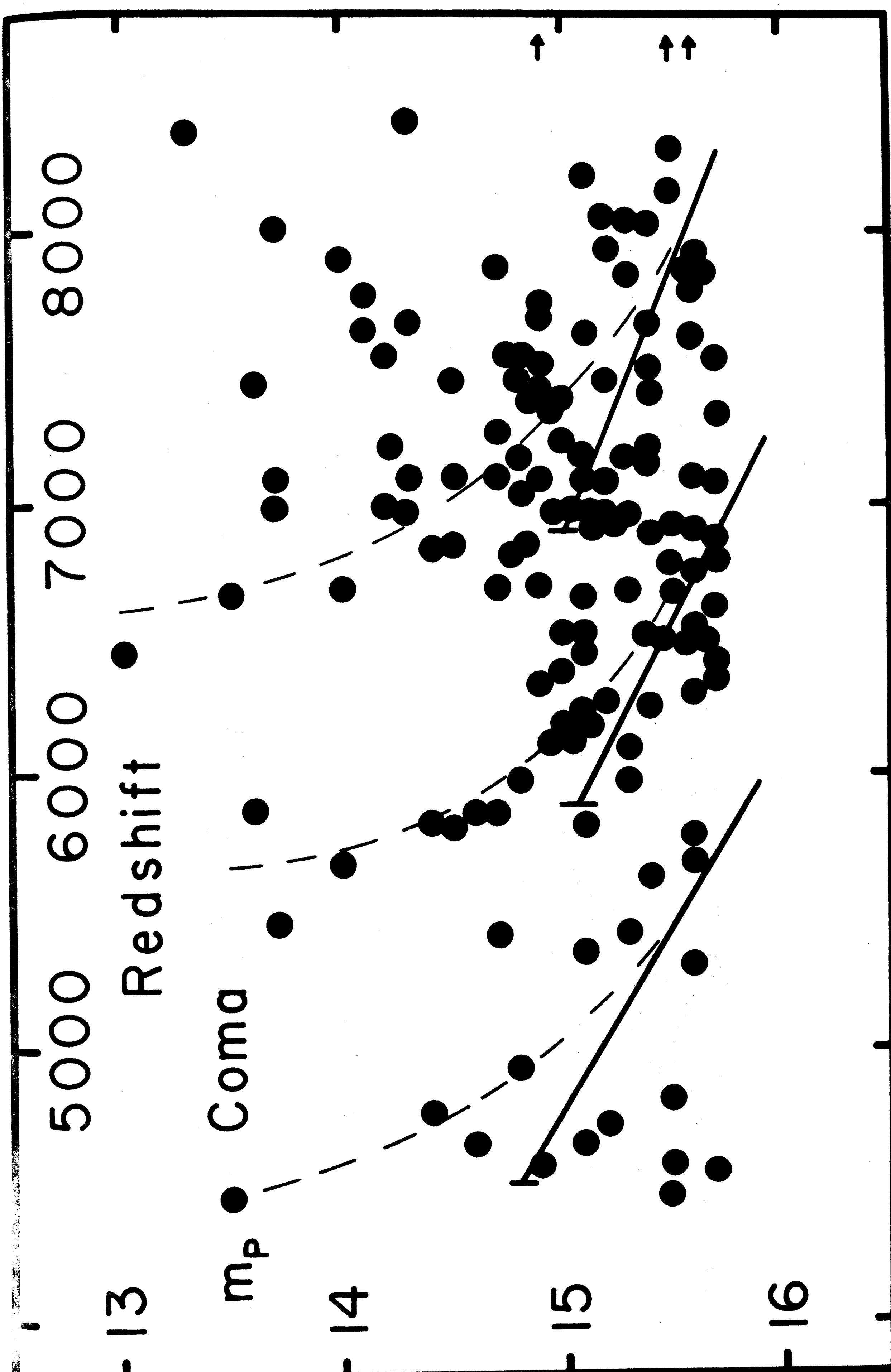

Redshift
Coma
m_P
5000
6000
7000
8000
13
14
15
16

FIGURE 13

The m_p-redshift diagram for the 10 identified 5C radio galaxies in the Coma cluster. The open circle refers to one double galaxy of less certain magnitude. The galaxies concentrate strongly in the high redshift range. The mean Coma redshift is shown by the arrow. The separation in redshift is unlikely at the 0.01 level if by accident. The galaxies occupy the one region of the diagram not associated with the primary bands.

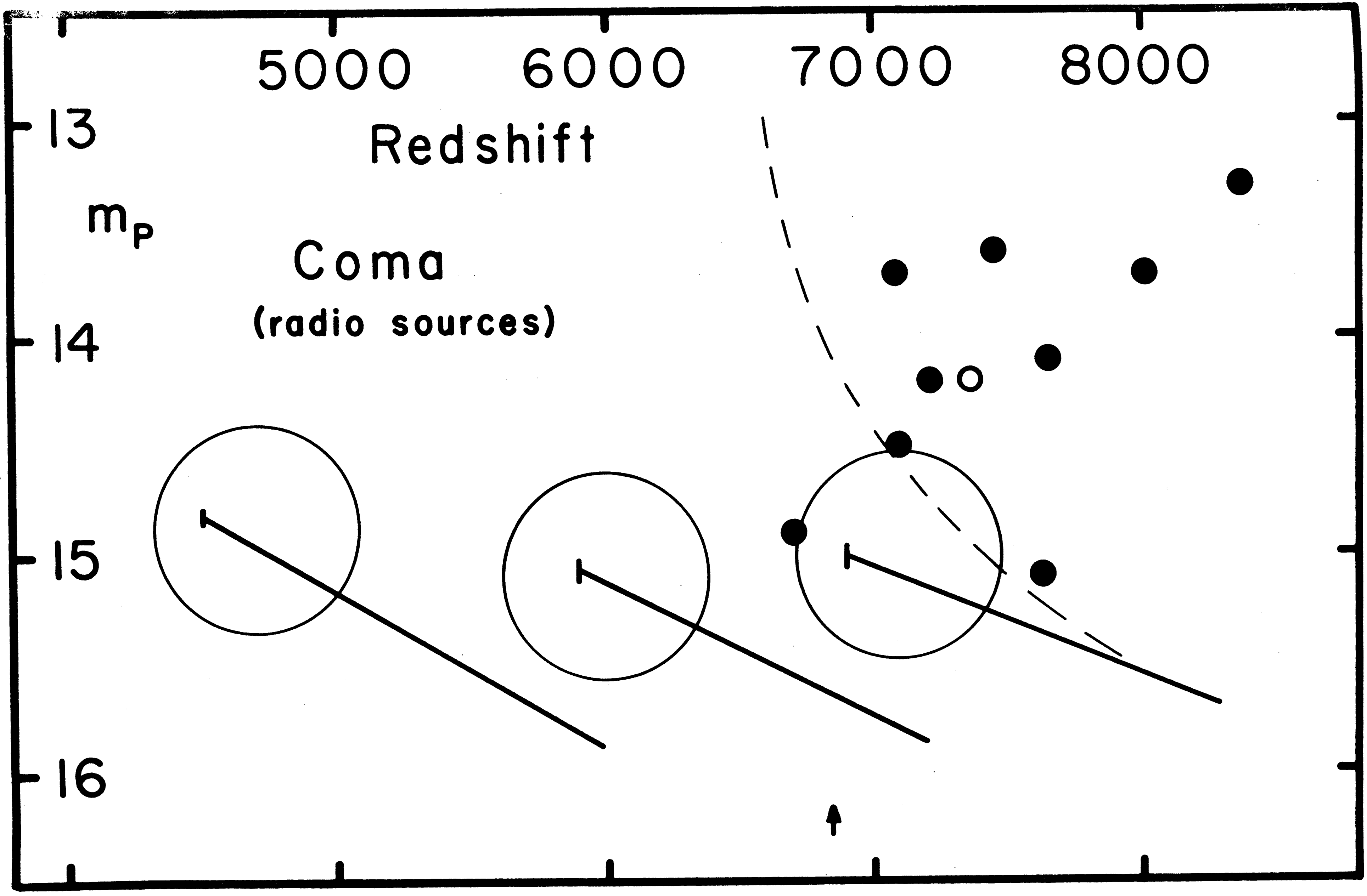
5000
6000
7000
8000
13
14
15
16
Redshift
m_P
Coma
(radio sources)

PREDICTIVE TESTING

The comparison of the inner and outer Coma cluster galaxies is one form of confirmation of the band concept. Because of the major differences in the equivalence of the samples the comparison is, however, more of an extension of the concept rather than an independent verification. Preliminary equivalent data on a second cluster, A2199, has been derived (Tifft 1972b), however, and is included here as a first full test of the band concept.

Table 4 contains redshifts and provisional nuclear region visual magnitudes for 34 galaxies within about 15 arc minutes of the center of the A2199 cluster. Galaxies are identified according to their numbers in the listing by Rood and Sastry (1972) or Minkowski (1961). Morphology and ellipticity is from Rood and Sastry (1972). Redshift source is Minkowski (1961), M, or new Steward Observatory 90-inch (225 cm) image tube spectra, C, obtained and measured in the same manner as those in the Coma cluster. One of the Minkowski redshifts (M17) has been revised (Minkowski, personal communication) and a second one (M7) is in question; otherwise, the comparison of redshifts is satisfactory with an average difference of 150 km sec^{-1}. The mean redshift of the cluster is 9061 km sec^{-1}. Magnitudes refer to the inner 3.6 arc second circular spot centered on the nucleus. The 3.6 arc second diameter has been chosen as equivalent to the 4.8 arc second region used in Coma after reduction in proportion to the greater redshift of the A2199 cluster. Except for RS50 for which a magnitude was estimated, the magnitudes were derived from image dissector scans of 90-inch calibrated V photographs and are unknown within a constant. Improved magnitudes as well as full details on the methods of derivation will be published subsequently. A comprehensive study of nearly 100 galaxies in the A2199 region is presently in progress.

In order to make a fully predictive test for the presence of banding in the A2199 cluster, we must specify the band slope and band spacing independently. Both of these properties can be inferred from Coma. Consider the band slope first. From Table 3 of CII the mean band slope of the nuclear magnitude bands was shown to be 3.25±0.1 magnitudes per factor of two in redshift. The slope, S, expressed in terms of magnitudes per 1000 km sec^{-1} of redshift will depend upon the mean redshift, $\overline{Vo}$, of the sample because of the band convergance toward zero redshift.

TABLE 4

Provisional Data for A2199

RS Number	M Number	Vo	V(3.6)+C	Type	ε	
50		8150 C	(15.4)	E	0.0	
52		8935 C	14.83	E	0.2	
56		9320 C	15.42	E	0.4	*
62		9338 C	15.44	SO	0.3	*
67		7875 C	15.26	SBO	0.0	
69		9323 C	15.45	E	0.3	*
76	1	9070 M	15.38	E	0.2	*
77	2	9690 M	15.24	SO	0.5	
80		9651 C	15.29	SO	0.3	
82		9350 C	15.48	SO	0.5	*
83	3	10480 MC	14.92	SO	0.6	
84		9548 C	15.54	SO	0.7	*
85	4	10090 M	15.92	SO	0.5	*
86	5	8674 MC	15.08	E	0.4	*
89	A	9480 M	15.57	D	0.3	*
	B	7960 M	15.34			
	C	10050 M	15.92			*
90	6	7730 MC	15.42	SB	0.3	
96	7	8376 C	15.37	SB	0.0	
97	8	10257 MC	15.94	SO	0.5	*
98	9	8318 MC	14.92	E	0.0	*
94	10	10740 M	15.06	SO	0.0	
	11	8780 M	15.86			
95	12	7851 MC	15.58	SO	0.8	
	13	8460 M	15.64			
	14	8396 MC	15.52			
	15	9297 MC	15.67			*
	16	8210 M	15.96			
99	17	9540 MC	15.18	SO	0.5	
104		9582 C	15.20	SBO	0.0	
109		8683 C	15.24	E	0.4	*
112	19	8802 MC	15.65	SO	0.4	
115		8771 C	14.80	SO	0.8	
116		8378 C	15.05	SBO	0.4	*

The relationship for S as a function of $\overline{V}o$ is

$$S \doteq 3250/\tfrac{2}{3}\overline{V}o = 4875/\overline{V}o. \qquad (1)$$

The band spacing as a function of $\overline{V}o$ may be inferred from Table 2 of CI by use of the formula, in CI notation,

$$\Delta Vo = (\Delta R/\sin\theta_o)\sigma_{Vo} \qquad (2)$$

to calculate individual spacings, and noting the typical Vo values at which this spacing occurs. In this manner we find the band 4-5 spacing is 1190 km sec^{-1} at $\overline{V}o \doteq 5700$, the band 5-6 spacing is 1130 km sec^{-1} at $\overline{V}o \doteq 6500$, and the band 6-7 spacing is 1050 km sec^{-1} at $\overline{V}o \doteq 7400$. These three values, along with the 1080 average Coma spacing at $\overline{V}o=6840$ define an approximate linear expression for band spacing as a function of $\overline{V}o$,

$$\Delta Vo \doteq 1680-0.085\overline{V}o. \qquad (3)$$

Using equations (1) and (3) and $\overline{V}o=9061$ for A2199 we infer that the nuclear magnitude band pattern in A2199 should occur at a mean slope of 0.54 magnitudes per 1000 km sec^{-1} of redshift and show a typical band spacing of 910 km sec^{-1}. Figure 14 shows the power spectrum of the A2199 sample projected at the predicted slope. The wavelength 910 km sec^{-1} falls precisely in the middle of a broad power peak of level 7. The probability of this situation occuring by accident is $e^{-7}=0.0009$. Figure 15 is the redshift-magnitude diagram of the A2199 sample. The predicted slope and spacing are shown. Note that A2199 also shows the progressively decreasing band spacing toward higher redshifts in accord with the variable spacing in Coma.

A somewhat similar predictive test was carried out in QI using the slope of the total magnitude bands in Coma to successfully predict a band direction for QSS objects. In this case the band spacing was not predicted since a completely different class of objects in a completely different redshift range was involved.

The other major correlations which the Coma investigations would predict for A2199 are the morphological separation in redshift and the direction of the morphological vector in the redshift-magnitude diagram. Table 5 summarizes the morphological properties of the cluster, and Figure 15 distinguishes the morphology where known. As Coma predicts the lower half of the redshift range is a mixture of E and non-E types, while the upper range is almost exclusively non-E galaxies. A Students'

FIGURE 14

Power spectrum of the A2199 cluster galaxy sample projected at a predicted slope of 0.54 magnitudes per 1000 km sec^{-1} of redshift and examined at a predicted wavelength of 910 km sec^{-1}. The high observed power at the specifically predicted slope and wavelength is unlikely at the 0.001 level if by accident.

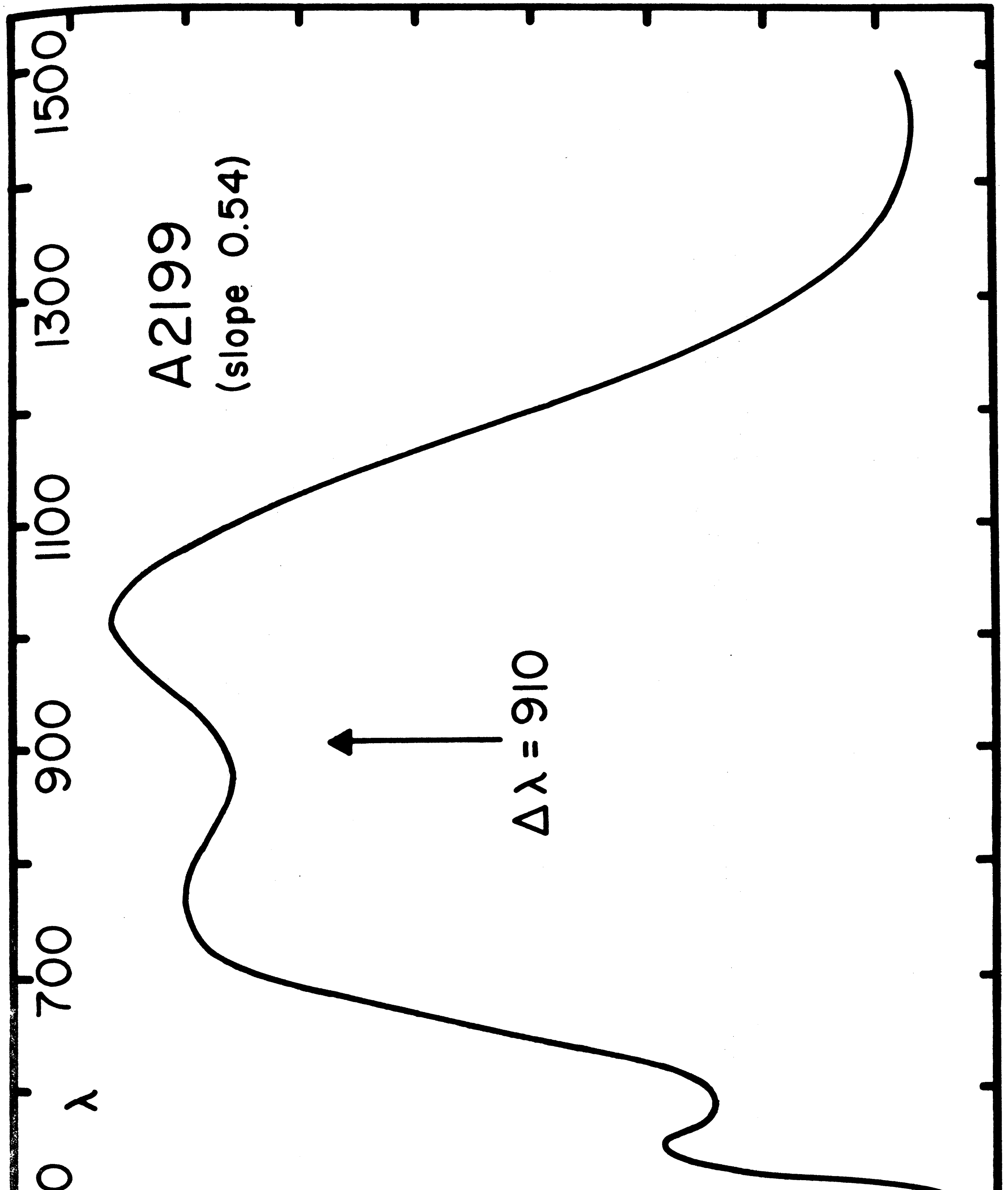
A2199
(slope 0.54)
Δλ = 910
λ
500
700
900
1100
1300
1500
P
1
2
3
4
5
6
7
8

FIGURE 15

The A2199 preliminary redshift-nuclear magnitude diagram. Filled circles are E galaxies, open circles are non-E types, and X symbols are unclassified galaxies. The mean redshift of the cluster is shown at the top. The pair of vectors at the lower right indicate the band direction and spacing predicted from Coma. The vector at the lower left gives the observed morphological separation direction. With regard to banding, morphological separation, and morphological direction, the A2199 cluster verifies the Coma pattern very closely.

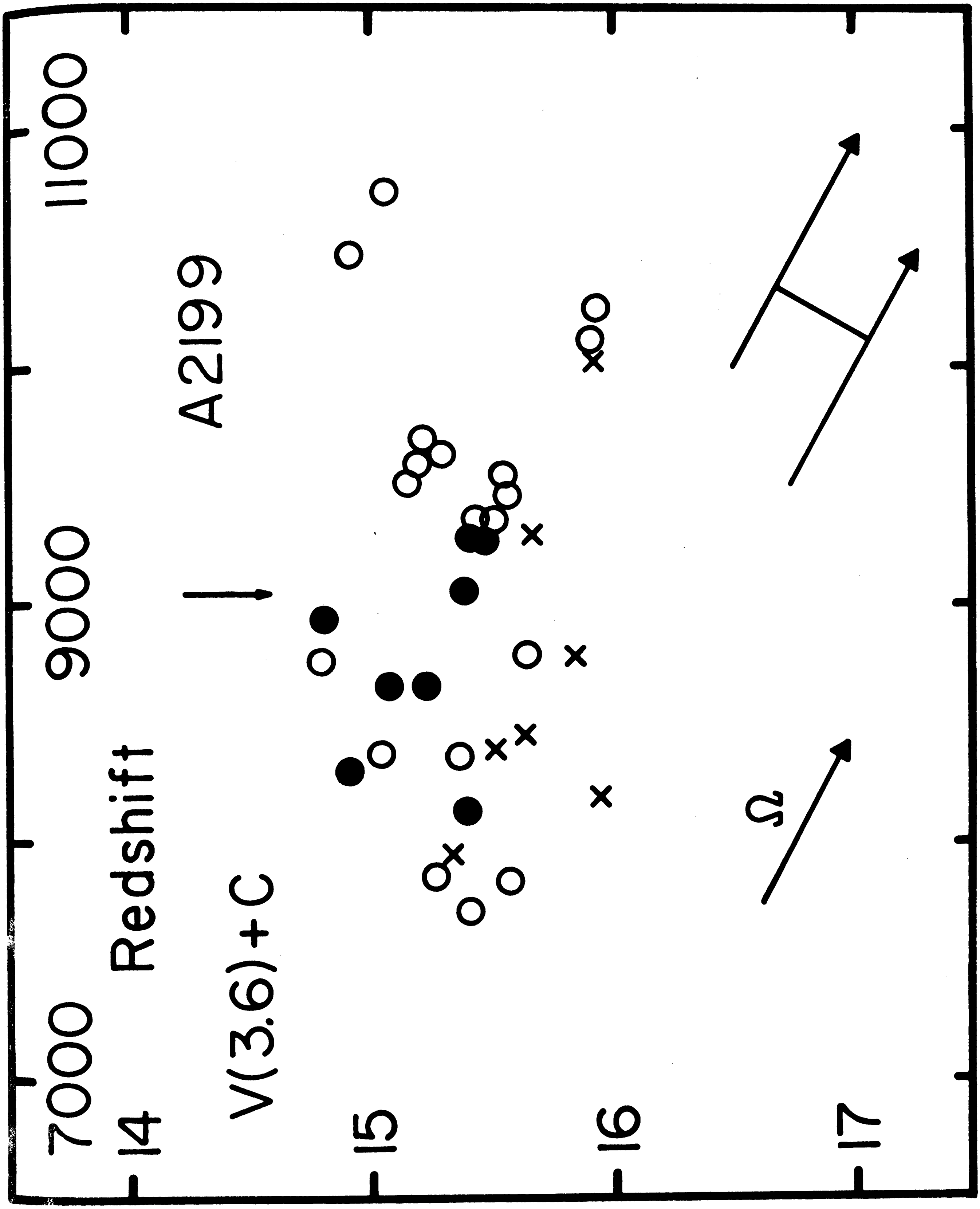
Redshift
7000
9000
11000
A2199
V(3.6)+C
14
15
16
17
Ω

t test on the separation of mean redshift by morphological types is not quite significant at t=1.3 (p=0.1) for the entire diagram. The separation is distinct and significant, however, on the one well defined band for which members are flagged in Table 4. We can conclude that while marginally significant by itself, the separation of morphology with redshift is in the same sense as Coma and can only constitute support for the band-morphology hypothesis. More striking than morphological separation is the morphological direction. For either the main band or the entire diagram (omitting RS50 of uncertain magnitude) the morphological slope S=0.51-0.52 is very close to the predicted S=0.54 band slope. In terms of the angle θ defined in CI the directions differ by less than 2°, which as for Coma is unlikely at the 0.02 level if accidental. Figure 15 contains the observed morphological vector.

TABLE 5

Properties of A2199 Galaxies

Type	No	$\overline{V(3.6)}$	$\overline{Vo}$	$\Delta m/\Delta Vo$	t(p)
E	7	15.19	8903	.00051	1.3(.1)
NE	19	15.36	9238		
*E	6	15.25	8898	.00052	2.1(.03)
*NE	7	15.56	9492		

Vo	No E	No NE	$\overline{\varepsilon}$
<9200	6	7	0.30
>9200	2	12	0.39
>9330	0	12	0.39

SUMMARY

All tests which have been applied to the redshift-magnitude banding phenomenon to date are consistant with interpretation of the entire redshift effect as an intrinsic property of matter. The reality of the phenomenon now rests on about 9 correlations and test, plus a number of other remarkable observations which defy assignment of probabilities of occurance by accident. The set of major independent correlations and tests with their "random likelihood" estimates, where available, are summarized in Table 6.

TABLE 6

Correlations and Tests of the Band Concepts

Correlations or Observations		Random Likelihood
1)	Existance of the Coma(70) bands in any direction	0.005
2)	Coma(70) morphological separation in redshift alone	0.01
3)	Agreement of Coma band and morphological directions	0.02
4)	Band convergence to zero redshift	?
5)	Organization of bands in a regular series	?
Predictions		
1)	m_p outer Coma SO redshift periodicity	0.03
2)	m_p outer Coma emission line galaxy redshift periodicity	0.02
3)	A2199 banding as predicted	0.001
4)	A2199 morphological separation in redshift alone	0.1 – 0.03
5)	Agreement of A2199 band and morphological directions	0.02
6)	QSS banding slope with no optimizing	0.02

REFERENCES

Barnothy, J. M. and Barnothy, M. F. 1973, Ap.J., original manuscript before revision.* BB

Burbidge, G. R. and Odell, S. L. 1972, Ap.J. 178, 583.

Chincarini, G. and Rood, H. J. 1972a, A.J. 77, 4.

____________. 1972b, ibid., 448.

____________. 1972c, PASP 84, 589.

Lake, R. G. and Roeder, R. C. 1972, JRAS Canada 66, 111.

Minkowski, R. 1961, A.J. 66, 558.

Rood, H. J. 1969, Ap.J. 158, 657.

Rood, H. J. and Baum, W. A. 1967, A.J. 72, 398.

Rood, H. J., Page, T. L., Kintner, E. C. and King, I. R. 1972, Ap.J. 175, 627. RPKK

Rood, H. J. and Sastry, G. N. 1972, A.J. 77, 451.

Tifft, W. G. 1972a, BAAS 4, 238.

________. 1972b, Steward Observatory Preprint No. 45.

________. 1972c, Ap.J. 175, 29. CI

________. 1973a, Ap.J. 179, 29. CII

________. 1973b, dito 181, 305. QI

Tifft, W. G. and Gregory, S. A. 1973, ibid., 15.

Willson, M. A. G. 1970, MNRAS 151, 1.

Zwicky, R. and Herzog, E. 1963, Catalogue of Galaxies and Clusters of Galaxies, Vol. II, Pasadena: California Institute of Technology.

* At the time of final acceptance of my paper fairly major revisions in the Barnothy and Barnothy paper were being contemplated and some of the material or statements referenced in my paper may not appear in their final form. Since the original material is quite representative of typical discussion relating to the reality of the band phenomena it is retained in the original for here, however.